

Tracer Testing at the Desert Peak EGS Project

Peter Rose¹, Kevin Leecaster¹, Peter Drakos², and Ann Robertson-Tait³

¹Energy and Geoscience Institute at the University of Utah

²Ormat Technologies, Inc.

³GeothermEx, Inc.

Keywords

Tracer testing, EGS, Desert Peak geothermal field, reservoir pore volume

ABSTRACT

As part of the Desert Peak EGS project, tracer testing was conducted involving two existing injection wells at the Desert Peak geothermal field. The tracer data showed very strong returns from both injectors to one of the production wells, with much lower returns to the remaining producers. The tracer-swept pore volume was estimated using a first-moment analysis of the return-curve data.

Introduction

The EGS project at Desert Peak, Nevada focuses on improving the injectivity of an unproductive well (27-15) on the northern boundary of the field. This well is completed within lithologies and a stress environment that render it a good EGS target well. Following a successful hydraulic stimulation, this well will allow for the mining of additional heat from the periphery of the field and enable more generation from an existing power plant.

In this paper, we present tracer data from a recent field study at the Desert Peak geothermal field. The purpose of the tracer testing was to characterize flow patterns between injection and production wells and to estimate the reservoir pore volume in anticipation of the hydraulic stimulation of target EGS well 27-15 on the northern boundary of the field. After the stimulation, the tracer testing will be repeated to determine changes in flow patterns and pore volume that occurred as a result of the stimulation.

Tracer Testing at Desert Peak

The uv-fluorescent naphthalene sulfonates have proven to be excellent tracers in high temperature geothermal reservoirs because they are environmentally benign, very detectable by fluorescence spectroscopy, affordable, and thermally stable. We have

studied eight of the naphthalene sulfonates in the laboratory and have found them to be suitable for use as conservative tracers in high temperature (>330°C) reservoirs (Rose *et al.*, 2001). Studies on surfactant toxicity indicate that these compounds are neither carcinogenic nor mutagenic (Greim *et al.*, 1994). Field tests in a number of geothermal reservoirs with temperatures up to 300°C further confirm the long-term stability of these chemicals.

On 11/6/2008, 85 kg of tracer 2,6-naphthalene disulfonate (2,6-nds) and 100 kg of tracer 1,5-naphthalene disulfonate (1,5-nds) were injected into wells 22-22 and 21-2, respectively (see Figure 1). Sampling of the five producing wells 21-1, 67-21, 74-21, 77-21, and 86-21 was initiated on 11/10/2008 and has continued through 2/23/2009. The samples were sent to the Tracer Development Laboratory at the University of Utah for analysis by liquid chromatography with fluorescence detection.

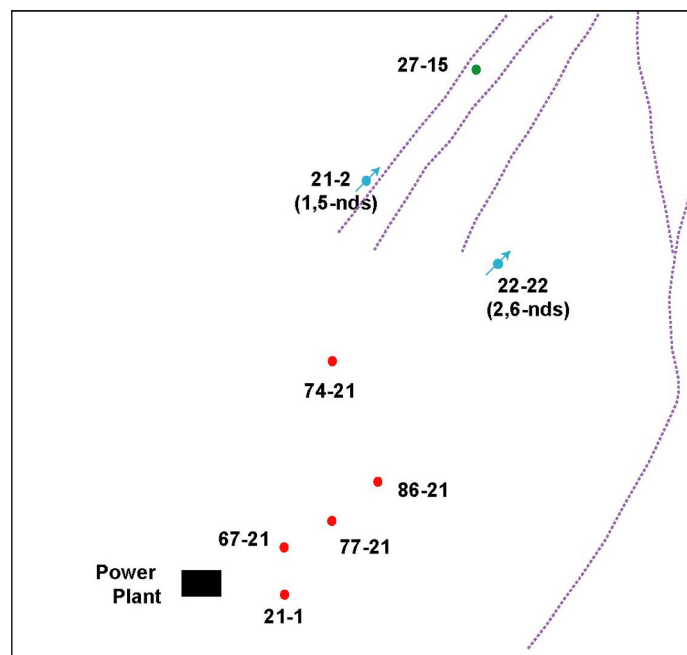


Figure 1. Map of the Desert Peak geothermal field.

The return of the two tracers to 74-21 (the closest producer to the south of the two injectors) was strong and immediate. Shown in Figure 2 is the return of tracer 2,6-nds from injector 22-22 and of tracer 1,5-nds from 21-2 to this production well as a function of time. It is evident that both the first arrival and the peak tracer concentration were missed for tracer 2,6-nds by the time the first sample was taken four days after tracer injection. The first arrival of tracer 1,5-nds to 74-21 again occurred before initial sampling of the well, but a peak concentration exceeding 250 ppb was observed approximately 6 days after injection. The well showing the next strongest returns was 67-21. Plotted in Figure 3 are the returns of tracer 2,6-nds from 22-22 and of tracer 1,5-nds from 21-2. The returns to 67-21 are delayed relative to the returns to 74-21. However, the maximum measured concentration of each tracer was less than one tenth of the maximum concentrations measured by either tracer in well 74-21.

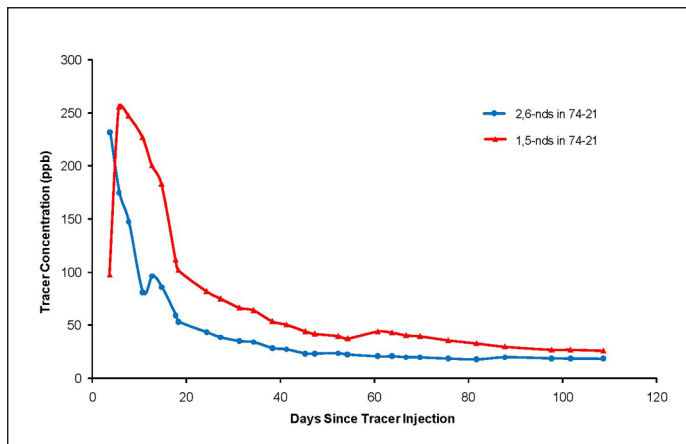


Figure 2. Return of tracers 2,6-nds and 1,5-nds from injection wells 22-22 and 21-2, respectively, to production well 74-21.

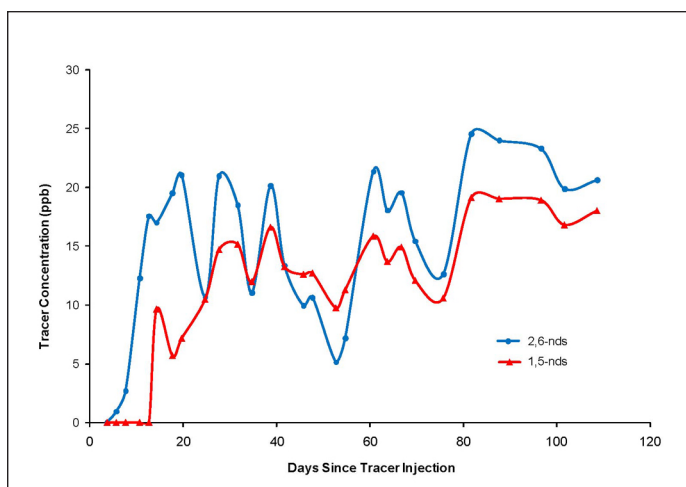


Figure 3. Return of tracers 2,6-nds and 1,5-nds from injection wells 22-22 and 21-2, respectively, to production well 67-21.

The well showing the next strongest returns was 77-21. Plotted in Figure 4 are the returns of tracer 2,6-nds from 22-22 and of tracer 1,5-nds from 21-2. The returns to 77-21 are delayed relative

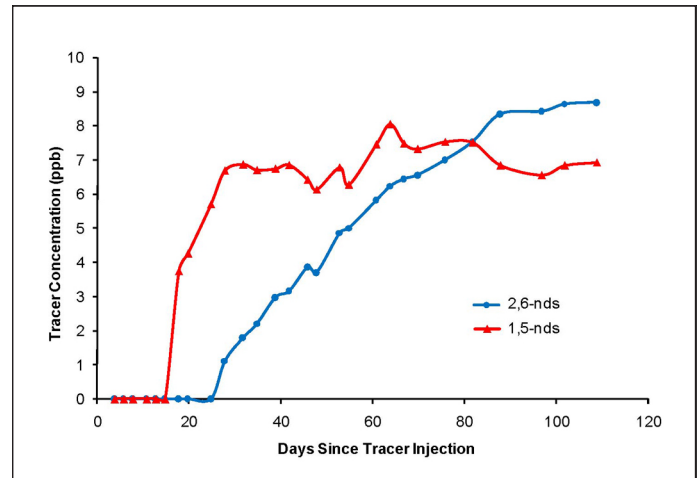


Figure 4. Return of tracers 2,6-nds and 1,5-nds from injection wells 22-22 and 21-2, respectively, to production well 77-21.

to the returns to 64-21, which, in turn, were delayed relative to the returns to 74-21. Likewise, the return curves of each tracer were diminished relative to the comparable curves plotted for 67-21 in Figure 3.

The well showing the lowest tracer concentrations was 86-21. Plotted in Figure 5 are the returns of tracer 2,6-nds from 22-22 and of tracer 1,5-nds from 21-2. These return curves represent the slowest first arrivals and the lowest concentrations of any of the monitored wells.

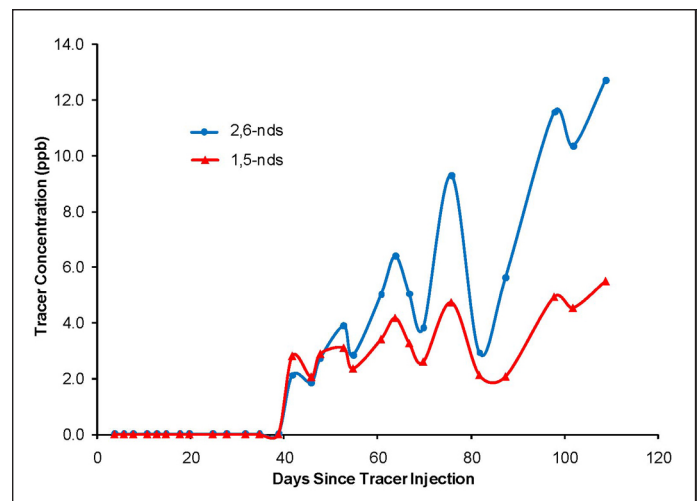


Figure 5. Return of tracers 2,6-nds and 1,5-nds from injection wells 22-22 and 21-2, respectively, to production well 86-21.

Finally, the tracer returns to all of the wells are plotted together in Figure 6. The most striking observation is that the returns of the two tracers to 74-21 were at least 10 times greater than those to any other well. Also, it is evident that the tracer concentrations decrease and the times for the first arrivals of peaks increase in progressing from 74-21 to 67-21 to 77-21 to 86-21. No tracer has yet been observed in samples taken from 21-1.

Figure 7 shows a conjectural flow pattern that accounts for the approximate relative concentration and arrival times of

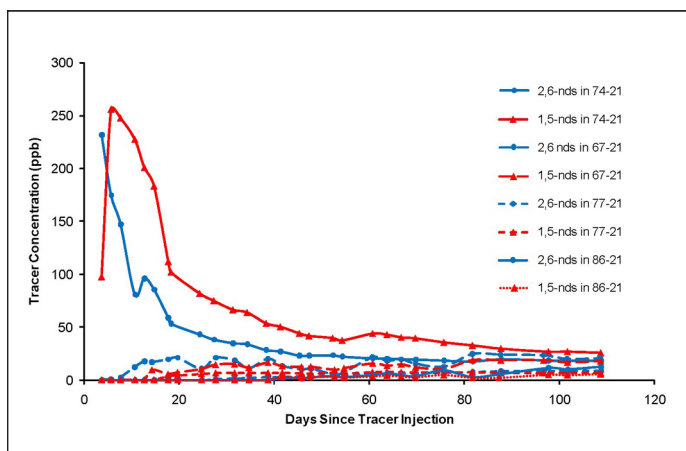


Figure 6. Return of tracers 2,6-nds and 1,5-nds from injection wells 22-22 and 21-2, respectively, to all production wells where tracer was observed.

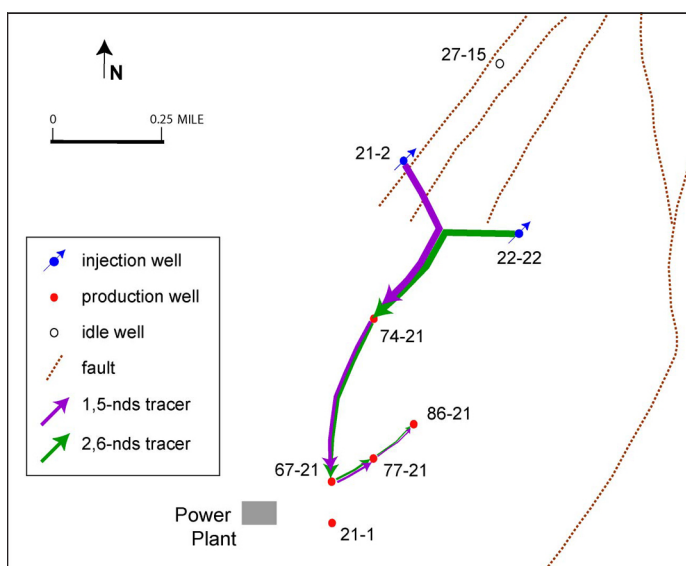


Figure 7. Conjectural flow pattern between injectors and producers at the Desert Peak field.

tracer between the two tagged injection wells and the production wells.

Estimation of Reservoir Pore Volume from Tracer Data

Tracer data have long been used by engineers to study fluid flow within continuous flow systems such as pipes and chemical reactor vessels. Danckwerts (1953) introduced the concepts of F-C diagrams and age distribution functions to characterize flow in a variety of patterns ranging from piston (segregated) flow to complete mixing. In addition, he demonstrated the use of moment analyses of tracer-test data to determine reactor-vessel volumes (Danckwerts, 1958).

Robinson (1985) applied the concepts of Danckwerts and others to the study of flow through fractured media and recognized two basic ways of defining pore volume based upon residence

time distribution (RTD) functions: modal volume and integral mean volume. The former corresponds to the maximum of the RTD curve and represents the volume of the primary (low impedance) fracture pathways. The latter is a more inclusive definition and represents the volume of all fractures, including both the low impedance and high impedance pathways.

Shook (2003) developed a proxy to true F-C diagrams based upon conservative-tracer data as a means of describing flow capacity and storage capacity in fractured media. He indicated that total pore volume could be obtained from the storage capacity proxy. In a later publication, Shook and Forsman (2005) described a method they developed to calculate reservoir pore volume from a first moment analysis of tracer data. Their method first involves a normalization of the tracer data to create a residence time distribution $E(t)$. Next, the data are deconvoluted to subtract the contribution made by tracer reinjection/recirculation, which, in turn, allows for a calculation of a true residence time distribution. Next, the return curve is extrapolated to long times, assuming an exponential decay of the long tailing portion of the return curve. This allows for a calculation of the true mean residence time, which then allows for a calculation of the interwell reservoir pore volume, V_p , according to the equation:

$$V_p = \frac{m}{M} \cdot Q \cdot t^*$$

where m is the mass of tracer recovered at the production well, M is the mass injected, Q is the flow rate into the injection well, and t^* is the true mean residence time, as described above.

The method and spreadsheet developed by Shook and Forsman (2005) were used to calculate the portion of the reservoir between injectors 22-22 and 21-2 and production well 74-21. The rest of the reservoir is excluded from the calculation. This approach was taken since, as shown in Figure 8, the overwhelming majority of circulation is between the two injectors and the closest producer, 74-21. The calculated pore volume was 50,000 m³ between 22-22 and 74-21 and 37,000 m³ between 21-2 and 74-21, for a total pore volume of 87,000 m³.

An assumption of the method of Shook and Forsman is that the long tailing portion of a deconvoluted tracer return curve decays exponentially. Shook (2005) showed that an exponential fit to the return curve from data from a Beowawe tracer test (Rose et al, 2004) gave the best fit. Even though the exponential fit is the best of the options studied, it still fails to match perfectly. Even a slight deviation from linearity (when plotted as a logarithm) of the return curve tail results in different pore-volume calculations as the tracer-test data are extended. As a result, for both the Beowawe (Rose, unpublished results) and Desert Peak tracer test data, the longer the deconvoluted return curve is extended, the greater the apparent pore volume.

Shown in Figure 8, overleaf, are plots of apparent pore volume as a function of tracer test duration for the 22-22 and 21-2 tests, respectively. Apparent pore volume between 22-22 and 74-21 increases from about 50,000 m³ to over 200,000 m³ as the duration of the tracer test is increased from 24 days to 108 days. Likewise, the apparent pore volume between 21-2 and 74-21 increased from about 37,000 m³ to about 88,000 m³ as the duration of the tracer test increased from 24 to 108 days. For each calculation, the lower value was chosen, since this was the region where the

long tailing portion of the returns curves most closely approached exponential decay.

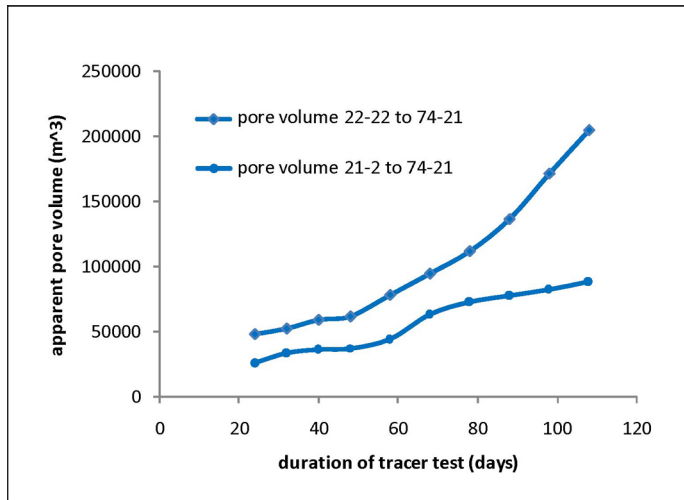


Figure 8. Apparent pore volume as a function of tracer-test duration for each of the tests.

Summary and Conclusions

Tracer testing was successfully conducted at the Desert Peak geothermal field. The purpose of the tracer testing was to characterize flow patterns between injection and production wells and to estimate the reservoir pore volume in anticipation of the hydraulic stimulation of target EGS well 27-15 on the northern boundary of the field.

Two mutually compatible naphthalene sulfonate tracers were injected into the two injection wells 22-22 and 21-2. The tracer data showed very strong returns from both injectors to one of

the production wells, with much lower returns to the remaining producers. A first moment analysis of the tracer data indicated a pore volume of approximately 87,000 m³ in the portion of the field separating the two injection wells and producer 74-21. After the stimulation of 27-15, the tracer testing will be repeated to determine changes in flow patterns and pore volume that occurred as a result of the stimulation.

Acknowledgments

This project was supported by the U.S. Department of Energy Office of Energy Efficiency and Renewable Energy under Cooperative Agreement DE-FC07-01ID14186. This support does not constitute an endorsement by the U.S. Department of Energy of the views expressed in this publication.

References

- Danckwerts, P. V. (1953) "Continuous Flow Systems: Distribution of Residence Times", *Chemical Engineering Science*, **2**(1), pp. 1-13.
- Danckwerts, P. V. (1958) "Local Residence Times in Continuous Flow Systems", *Chemical Engineering Science*, **9**, pp. 78-79.
- Rose, P.E., Mike Mella, Christian Kasteler, and Stuart D. Johnson (2004) "The Estimation of Reservoir Pore Volume from Tracer Data", SGP-TR-175, *Proceedings, Twenty-ninth Workshop on Geothermal Reservoir Engineering*. Stanford University, Stanford, California.
- Shook, G.M. (2003) A Simple, Fast Method of Estimating Fractured Reservoir Geometry from Tracer Tests, *Geothermal Resources Council Transactions*, **27**, pp. 407-411.
- Shook, G.M. and Forsman, J.H. (2005) Tracer Interpretation Using Temporal Moments on a Spreadsheet, INL/EXT-05-00400.
- Shook, G.M., (2005) "A Systematic Method for Tracer Test Analysis: An Example Using Beowawe Tracer Data" SGP-TR-176, *Proceedings, Thirtieth Workshop on Geothermal Reservoir Engineering*. Stanford University, Stanford, California.

Cost of Electric Power from Enhanced Geothermal Systems — Its Sensitivity and Optimization

Subir K. Sanyal

GeothermEx, Inc.
Richmond, California
mw@geothermex.com

Keywords

Enhanced Geothermal Systems, EGS, economic optimization

ABSTRACT

Based on a review of the Enhanced Geothermal Systems (EGS) developed to date worldwide, numerical simulation of idealized EGS reservoirs, economic sensitivity analysis, and practical considerations of some site characteristics, this paper shows that certain steps can be taken towards minimizing the levelized cost of electric power from EGS systems; these steps are as follows: (a) choosing the site with the highest possible vertical temperature gradient and for the thickest possible sedimentary cover on the basement; (b) choosing the drilling depth that maximizes a well's power capacity per unit drilling cost rather than reaches the hottest resource; (c) creating the largest possible stimulated volume per well; (d) increasing per well productivity by stimulating multiple, "vertically stacked" zones and/or increasing the pumping rate of production wells taking advantage of the evolving advances in pump technology; (e) improving stimulation effectiveness, and particularly, reducing the fracture spacing and heterogeneity in the hydraulic characteristics of the stimulated volume; (f) through reservoir modeling, optimizing well spacing and injection rates that minimize the rate of decline in net generation with time (g) reducing the power plant cost; (h) developing multiple, contiguous EGS units to benefit from the economy of scale; and (i) reducing the operations and maintenance cost. The basis for these conclusions is presented in the paper.

Introduction

Enhanced Geothermal Systems ("EGS") are hydraulically tight reservoirs whose permeability has been enhanced by hydraulic stimulation. An EGS "unit" in this paper refers to an injection well and the neighboring production wells that derive fluid from it; for example, a doublet, triplet, five-spot, etc. The reservoir is assumed to be developed in the basement rock rather than in any sedimentary overburden. Most of the parameters in this exercise

reflect the conditions encountered at the Desert Peak EGS project in the U.S. and the costs reflect 2006 U.S. dollars, but the conclusions reached here regarding optimization should be applicable, at least qualitatively, to most EGS projects today.

Optimization of geothermal resource economics calls for minimizing the levelized cost of power ($\text{\$}$ per kilowatt-hour) over the project life. Minimizing the levelized cost, in turn, requires minimizing the capital cost of project development ($\text{\$}$ per kilowatt-hour installed) as well as the operations-and-maintenance ("O&M") cost ($\text{\$}$ per kilowatt-hour generated). In this study, the levelized cost of power is defined as the cumulative present value of all costs incurred in generating the cumulative electricity over the life of the plant; the amount of electricity generated in a future year has not been discounted to the present because the assumption of a discount factor would be entirely arbitrary. As such, the levelized cost as defined in this paper may be considered the lowest possible estimate of the levelized cost. The general approach in this study was as follows: (a) using numerical simulation of idealized EGS reservoirs to estimate power generation over time for various system configurations (number and spacing of wells, assumptions about stimulation effectiveness, etc.); (b) estimating the levelized power cost for each configuration, based on capital cost, O&M cost, cost of money and inflation rate; (c) determining the sensitivity of levelized cost to the cost components, interest and inflation rates, and resource characteristics (pumping rate, reservoir properties, depth to the reservoir, etc.); and (d) based on this sensitivity analysis and certain issues of site characteristics, identifying the practical steps that could be taken towards economic optimization.

Choosing the EGS Site

It is obvious that the higher the vertical temperature gradient, that is, the higher the heat flow rate at the surface, the more attractive the site should be. Sanyal and Butler (2004) presented an approach to estimating the EGS resource base using heat flow estimates at the surface. Using this approach, Figure 1, overleaf, presents estimates of potential EGS power capacity per square mile versus drilling depth for a range of surface heat flow values,

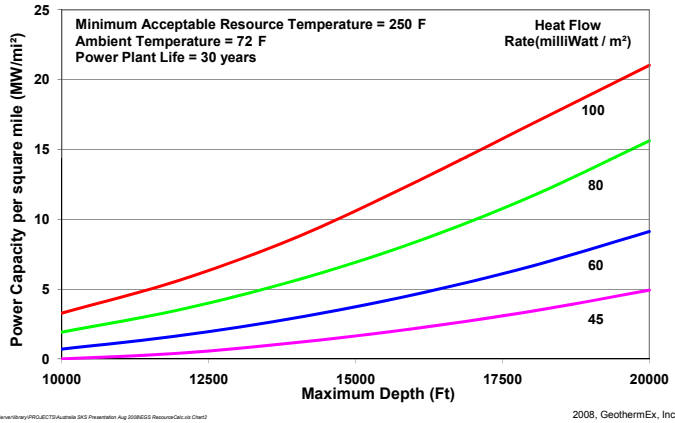


Figure 1. EGS Resource Base versus Drilling Depth.

assuming a minimum acceptable resource temperature of 250°F for power generation, a power plant rejection temperature of 72°F and a plant life of 30 years.

As to be expected, the power capacity increases nearly exponentially with depth, and more steeply for higher heat flow rates (Figure 1). However, drilling cost also increases nearly exponentially with depth. Using the drilling cost versus depth correlation presented in Sanyal et al (2007a), we can estimate the reserves potentially secured per million dollar drilling cost for any drilling depth. Figure 2 presents the estimated potential reserves secured per million dollar drilling cost as a function of depth for various heat flow values, the other assumptions being the same as for Figure 1.

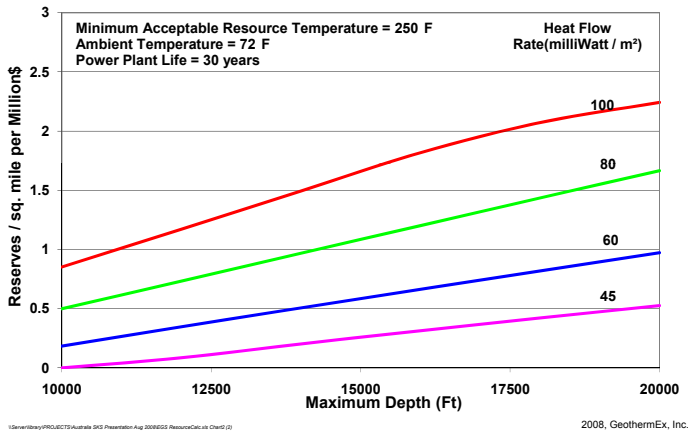


Figure 2. Reserve per Square Mile per Million \$ Drilling Cost.

This figure shows that the potential reserves per unit drilling cost does not go up exponentially but tends to flatten out with depth, particularly for high heat flow rates. In other words, deeper drilling to secure a larger reserve base does not necessarily lead to economic optimization.

Site selection is often based on regional heat flow distribution and drilling of relatively shallow exploration wells. However, the temperature gradient measured at relatively shallow depths cannot be extrapolated downward indefinitely because of intervening geological issues such as the thickness of sediment cover on the basement, lithology changes, radioactive heat generation in the basement or the presence of natural convection cells. For example,

Figures 3 and 4 show examples of the effects of the thickness of sediment cover and radioactive heat generation, respectively, on the deep temperature gradient.

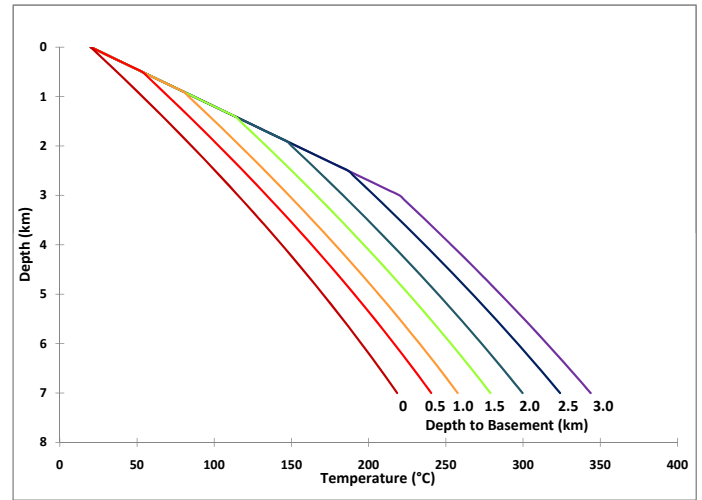


Figure 3. Effect of Depth to Basement on Temperature Profile.

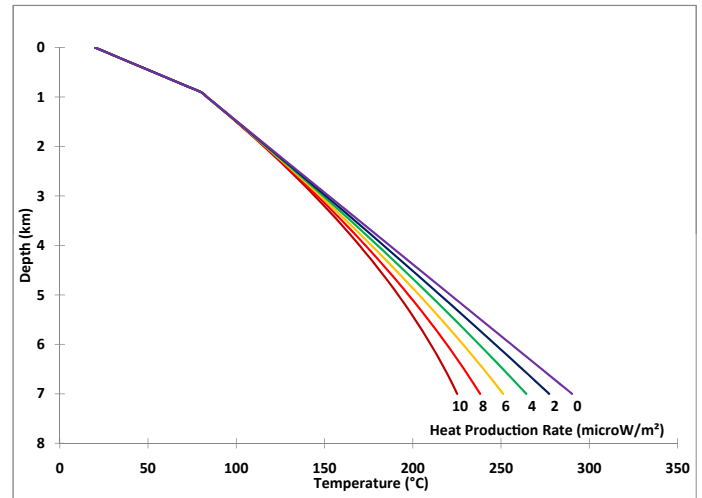
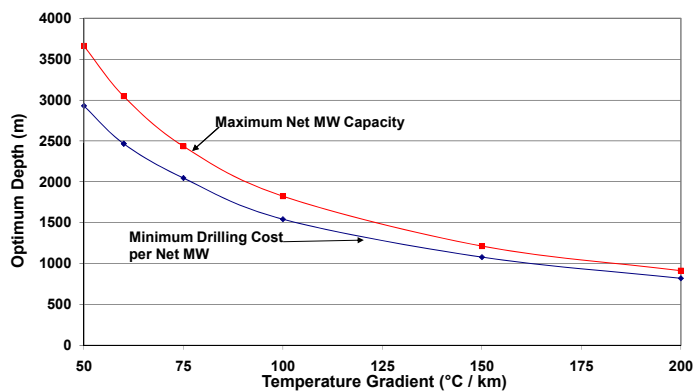


Figure 4. Effect of Radioactive Heat Generation on Temperature Profile.

While energy reserves per unit area at any site increases with depth, net MW production capacity per well does not necessarily increase with depth (Sanyal et al, 2007b). This issue arises from the fact that up to the depth where the temperature reaches 190°C, which is generally the temperature limit for pumps available today, the capacity of a pumped well would increase with depth. Below this depth a well will have to be self-flowed and its capacity would actually be less; this would be true up to the depth where the temperature reaches about 220°C. Above this temperature level no generalization is possible about well capacity. Sanyal et al (2007b) showed that considering the maximum well capacity achievable and cost of drilling versus well depth, an optimum drilling depth may be defined, in theory at least, at a site; this optimum drilling depth can be either the depth at which the well capacity is maximized or the drilling cost per MW well capacity minimized (Figure 5).



\\Server\library\PROJECTS\Australia SKS Presentation Aug 2008\NetMWCapac\Drilling.xls Chart6

2007, GeothermEx, Inc.

Figure 5. Optimum Drilling Depth of an EGS Project versus Temperature Gradient.

Consideration of Reservoir Performance

Performance of EGS systems is typically judged by the cooling trend of the produced water, with faster cooling rates representing less attractive performance. However, from a practical viewpoint, we believe that the net electric power capacity available from such a system versus time, defined in Sanyal and Butler (2005) as the “net generation profile,” is a more appropriate and comprehensive criterion of performance. Numerical simulation shows that, for any fracture spacing, fracture permeability and production/injection well configuration, reducing the throughput (that is, injection and production rates) reduces the temperature decline rate and lowers parasitic losses, thus resulting in a more commercially attractive net generation profile (that is, one with a lower variance). Heat recovery is less for a lower production rate, but due to reduced parasitic loads and a longer producing life, the net MW-hours supplied is greater than for cases with higher throughputs. One can arrive at an optimized net generation profile through numerical reservoir simulation by trial-and-error adjustment to the throughput. It may be argued that a declining net generation profile rather than a flat one may allow faster recovery of capital initially, and as such, may prove more attractive commercially. We have assumed up to a 15% variance in the net generation profile to allow for this possibility.

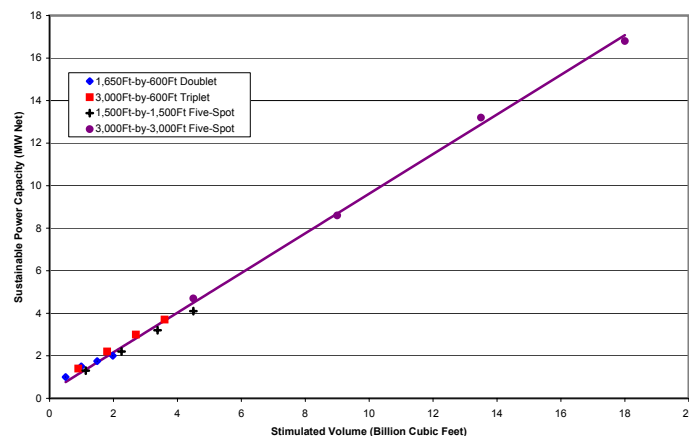
In numerical simulation, we have assumed that after stimulation, the fracture characteristics will remain unchanged over the project life. While enhancement of fractures with time due to thermal contraction of rock is possible, gradual closing of fractures or degradation of fractures due to scaling is also possible. Case histories of long-term injection into hydrothermal reservoirs do not show convincing or consistent evidence of progressive fracture enhancement with time, while degradation of fracture characteristics due to scaling with time is uncommon. Therefore, a fracture system that is invariant with time was considered a reasonable compromise for this exercise. To study the performance of a hypothetical EGS project similar to the Desert Peak project, we had developed earlier a three-dimensional, double-porosity numerical model (Sanyal and Butler, 2005); we have modified that model as needed for this analysis.

From the forecast of the production rate and temperature from the reservoir model, the net power generation versus time was calculated, for each well geometry, after subtracting the parasitic

power needed by injection and production pumps as a function of time as the produced water cools. For each combination of assumed geometry, injector-producer spacing, stimulated thickness, enhancement level (fracture spacing and permeability) and production rate, three criteria of performance were computed: (a) net generation profile (net generation versus time over project life), (b) net power produced per unit injection rate, and (c) fraction of in-place heat energy recovered.

This numerical simulation study led to the following conclusions relevant to optimization of resource economics:

- Cooling rate at production wells is not an adequate criterion for measuring the effectiveness of an EGS power project; net generation profile and reservoir heat recovery factor are more appropriate criteria.
- Improving permeability, without improving the matrix-to-fracture heat transfer area (that is, reducing the fracture spacing), has little benefit in heat recovery or net generation.
- The net generation profile can be improved (that is, the decline rate can be reduced) by curtailing the throughput without substantially affecting average generation over the project life.
- Increasing the stimulated volume increases the generation level without significantly affecting the shape of the generation profile.
- For a given state of stimulation (that is, fracture spacing and permeability) average net generation increases linearly with stimulated volume and is nearly independent of well geometry (Figure 6).



2009, GeothermEx, Inc.

Figure 6. Sustainable Power Capacity versus Stimulated Volume (from Sanyal and Butler, 2005).

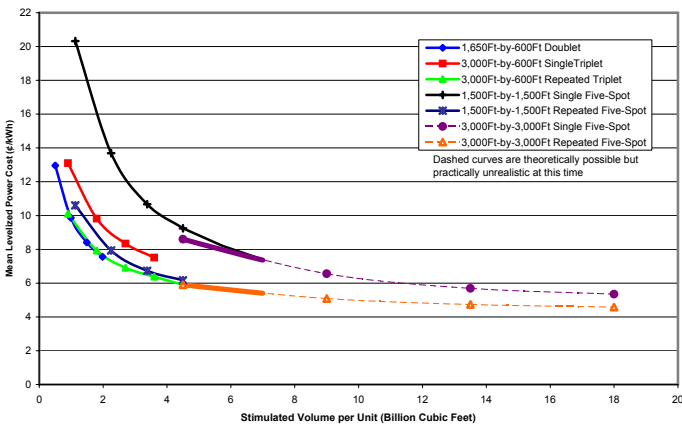
Economic Issues

This analysis has utilized the economic model presented by Sanyal et al (2007a). We have estimated the drilling cost based on a statistical correlation with depth, and the stimulation cost based primarily on the experience of the European EGS project at Soultz-sous-Forêts and Geodynamics’ EGS project at Cooper Basin, Australia. For the power plant and surface facilities cost and the O&M cost, we have used the typical range of values in the U.S. geothermal industry. The uncertain variables in this analysis

(capital costs of drilling, stimulation, power plant and surface facilities, O&M cost, interest rate and inflation rate) were subjected to Monte Carlo sampling and used in a probabilistic assessment of the levelized power cost. The capital cost was amortized over the project life at the assumed interest rate, and O&M cost was increased at the inflation rate over the project life. The annual capital-plus-interest payment and O&M cost were discounted to their present value using the inflation rate. The mean levelized power cost versus stimulated volume per EGS unit was thus estimated for many configurations and various stimulated volumes considered.

The economic analysis resulted in the following conclusions relevant to economic optimization:

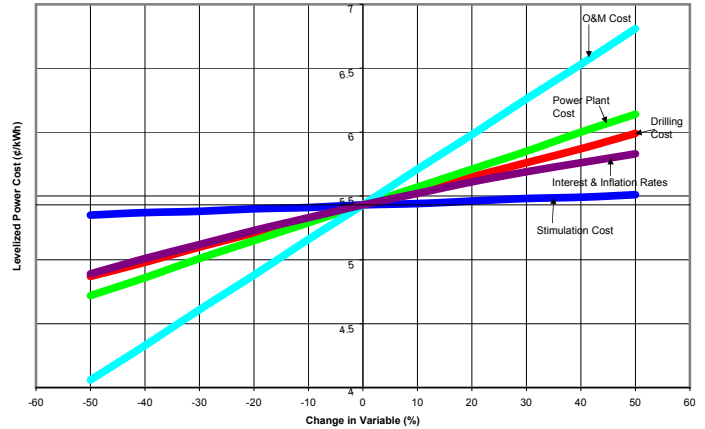
- (a) Levelized power cost declines with increasing stimulated volume, and for any configuration, with the repeating of contiguous EGS units (Figure 7).



2009, GeothermEx, Inc.

Figure 7. Mean Levelized Cost of EGS Power versus Stimulated Volume (from Sanyal et al, 2007a).

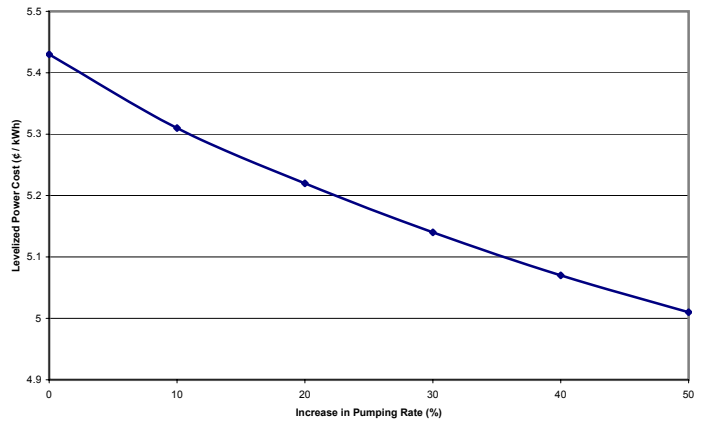
- (b) The lowest possible levelized cost of power at Desert Peak, under ideal conditions, was estimated at 5.43¢ per kWh (2006 \$), ignoring certain uniquely site-specific and/or atypical costs of exploration, infrastructure development (such as roads and the transmission line), regulatory compliance, environmental impact mitigation, royalties, and taxes.
- (c) Levelized power cost for the case considered is most sensitive to O&M cost, followed by power plant/surface facilities cost, per well productivity, drilling cost per well and interest/inflation rates, in that order (Figure 8). This order of sensitivity is likely to be somewhat site-specific, particularly as regards drilling, O&M and per-well production rate. Levelized cost is insensitive to stimulation cost but very sensitive to the effectiveness of stimulation (Figure 8), which cannot be readily quantified in such an economic analysis.
- (d) Improvements in geothermal pump technology in the future could allow increasing the maximum practicable pumping rate from a well (currently 200 l/s), thus reducing the levelized power cost; a plausible 50% improvement in the pumping rate can reduce the levelized cost by 0.43¢/kWh. Productivity per well can be increased for self-flowing wells by stimulating multiple “vertically stacked” zones.



2009, GeothermEx, Inc.

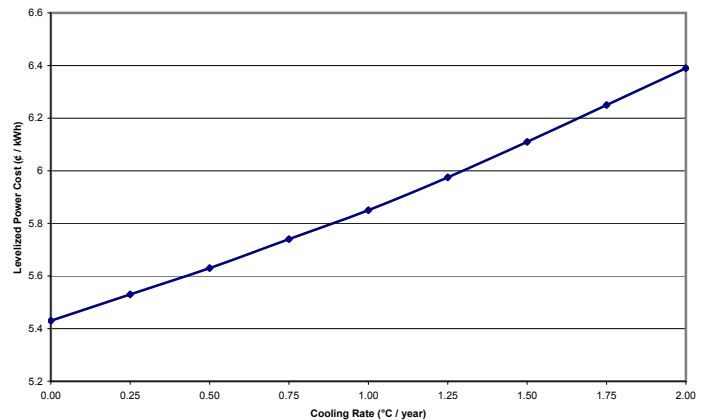
Figure 8. Sensitivity of Levelized Power Cost.

- (e) The effectiveness of stimulation in creating closely-spaced fractures and the desired reservoir characteristics (uniform, isotropic and sub-horizontal) reduces the risk of cooling of the produced fluid. The levelized power cost is sensitive to cooling rate; each °C per year increase in cooling rate increases the levelized power cost by 0.5¢/kWh (Figure 9).



2009, GeothermEx, Inc.

Figure 9. Levelized Power Cost versus Cooling Rate (from Sanyal et al, 2007a).



2009, GeothermEx, Inc.

Figure 10. Levelized Power Cost versus Well Depth (from Sanyal et al, 2007a).

- (f) Reservoir depth determines drilling cost, energy reserves and well productivity, while the effectiveness of stimulation, which is dependent on the lithology and in-situ stress condition at the site, determines cooling.

Therefore, the levelized cost can be very sensitive to site characteristics. Figure 10 shows the sensitivity of levelized power cost to well depth.

Conclusions

Based on the options in choosing the site, consideration of reservoir performance and economic analysis we conclude that the following steps can be taken towards minimizing the levelized cost of EGS power:

- (a) Choose the site with the highest possible vertical temperature gradient and/or the thickest possible sedimentary cover on the basement.
- (b) Choose the drilling depth that maximizes a well's power capacity per unit drilling cost rather than reaches the hottest resource.
- (c) Create the largest possible stimulated volume per well.
- (d) Increase per well productivity by stimulating multiple "vertically stacked" zones and/or increasing the pumping rate of production wells taking advantage of the evolving advances in pump technology.
- (e) Improve stimulation effectiveness, and in particular, reduce the fracture spacing and heterogeneity in the hydraulic characteristics of the stimulated volume.
- (f) Through reservoir modeling optimize well spacing and injection rates that minimize the rate of decline in net generation with time.
- (g) Reduce the power plant cost.
- (h) Develop multiple, contiguous EGS units to benefit from the economy of scale.
- (i) Reduce the operations and maintenance cost.

References

- Sanyal, S.K. and S.J. Butler, (2004), "National Assessment of U.S. Enhanced Geothermal Resource Base – A Perspective," Geothermal Resources Council Transactions, Vol. 28.
- Sanyal, S.K. and S.J. Butler, (2005), "An Analysis of Power Generation Prospects From Enhanced Geothermal Systems," Geothermal Resources Council Transactions, Vol. 29.
- Sanyal, S.K., J.W. Morrow, S.J. Butler and A. Robertson-Tait, (2007a), "Is EGS Commercially Feasible?," Geothermal Resources Council Transactions, Vol. 31.
- Sanyal S.K., J.W. Morrow, and S.J. Butler, (2007b), "Geothermal Well Productivity: Why Hotter is Not Always Better," Geothermal Resources Council Transactions, Vol. 31.